European Journal of Radiology 82 (2013) e142–e150

Contents lists available at SciVerse ScienceDirect

European Journal of Radiology

journal homepage: www.elsevier.com/locate/ejrad

Accuracy of low-dose computed tomography (CT) for detecting and characterizing the most common CT-patterns of pulmonary disease

Andreas Christe[a,b,*], Jaled Charimo-Torrente[b,1], Kingshuk Roychoudhury[c,2], Peter Vock[b,1], Justus E. Roos[a,3]

[a] Department of Radiology, Stanford University Medical Center, 300 Pasteur Drive, Stanford, CA 94305, USA
[b] Department of Interventional, Pediatric and Diagnostic Radiology, Inselspital, University Hospital, University of Bern, Freiburgstrasse 10, 3010 Bern, Switzerland
[c] Statistics Department, University College Cork, Cork, Ireland

ARTICLE INFO

Article history:
Received 25 June 2012
Received in revised form
26 September 2012
Accepted 27 September 2012

Keywords:
Low-dose CT
Common CT patterns
Lung nodules
Chest CT

ABSTRACT

Purpose: To assess the ability of low-dose CT to detect and characterize the most common CT patterns of pulmonary disease.
Methods and materials: Sixty patients with nodules, consolidations or interstitial disease were scanned using a low-dose (128 mm × 0.6 mm, 40 reference mAs, 120 kVp) and standard-dose CT protocol (150 reference mAs, 120 kVp). Two radiologists with 3 and 10 years of thoracic imaging experience searched both exams in consensus for the most commonly observed CT patterns according to the Fleischner Society criteria, which consisted of 46 different subgroups of ground-glass opacities, nodules, interstitial and airspace diseases. The standard of reference was established by consensus of a panel of two experienced chest radiologists (9 and 12 years of experience).
Results: The lung segments (1080) showed 813 nodules, 596 ground-glass opacities, 74 airspace and 575 interstitial diseases and 64 normal segments. In particular, air-space disease and nodules were unaffected by the increase in noise. However, the sensitivity to detect ground-glass opacities, ground-glass nodules and interstitial opacities decreased significantly, from 89% to 77%, 86% to 68% and 91% to 71%, respectively (all p-values < 0.00001). Using iterative reconstruction instead of the applied filtered back projection sensitivity for ground-glass nodules rose to the sensitivity of standard-dose CT in an additional phantom study.
Conclusion: A low-dose CT of 40 mAs/120 kVp is feasible for detecting solid nodules, airspace, airways and pleural disease. For diagnosing pathologies consisting of ground-glass opacities or interstitial opacities, higher tube current or iterative reconstruction is required.
© 2012 Elsevier Ireland Ltd. All rights reserved.

1. Introduction

Lowering tube current as a means of reducing radiation dose during CT examinations has been proven effective, showing no significant loss in objective or subjective diagnostic image quality [1–8]. By injecting noise into the acquired raw CT data, simulation studies were capable of testing a wide tube-current range to determine lowest and/or optimal dose levels for detecting specific lung abnormalities [5,6], with the added advantage of not exposing patients to additional radiation doses. A lowest acceptable tube current-time of between 5 mAs and 43 mAs has been proposed, i.e., for lung nodule detection, that maintains a sensitivity comparable with standard-dose chest CT applied at 100–250 mAs [9,10]. Other studies have investigated even further and in addition to investigating dose-dependent detection rates, have examined changes in non-nodular CT patterns relative to the simulated tube-current reductions. Although the detection rate of solid nodules remained constant at the lowest tube-current possible (10 mAs), Christe et al. [8] demonstrated that for discrimination of nodular patterns, such as subsolid nodules that occur in fungal pulmonary infections, dose levels of at least 30 mAs were required. Thus, the

* Corresponding author at: Department of Radiology, University Hospital of Bern, Inselspital, Freiburgstrasse 10, CH-3010 Bern, Switzerland. Tel.: +41 31 6321965; fax: +41 31 6324874.
E-mail addresses: andreas.christe@insel.ch, andreas.christe@hotmail.com (A. Christe), jaled.charimotorrente@insel.ch (J. Charimo-Torrente), kingshuk.roy.choudhury@duke.edu (K. Roychoudhury), peter.vock@med.unibe.ch (P. Vock), justus.roos@ksw.ch (J.E. Roos).
[1] Department of Radiology, University Hospital of Bern, Inselspital, Freiburgstrasse 10, CH-3010 Bern, Switzerland. Tel.: +41 316322111; fax: +41 31 6324874.
[2] Tel.: +353 0 21 420 5892; fax: +353 0 21 420 5367.
[3] Tel.: +41 52 266 41 19; fax: +41 52 266 45 09.

0720-048X/$ – see front matter © 2012 Elsevier Ireland Ltd. All rights reserved.
http://dx.doi.org/10.1016/j.ejrad.2012.09.025

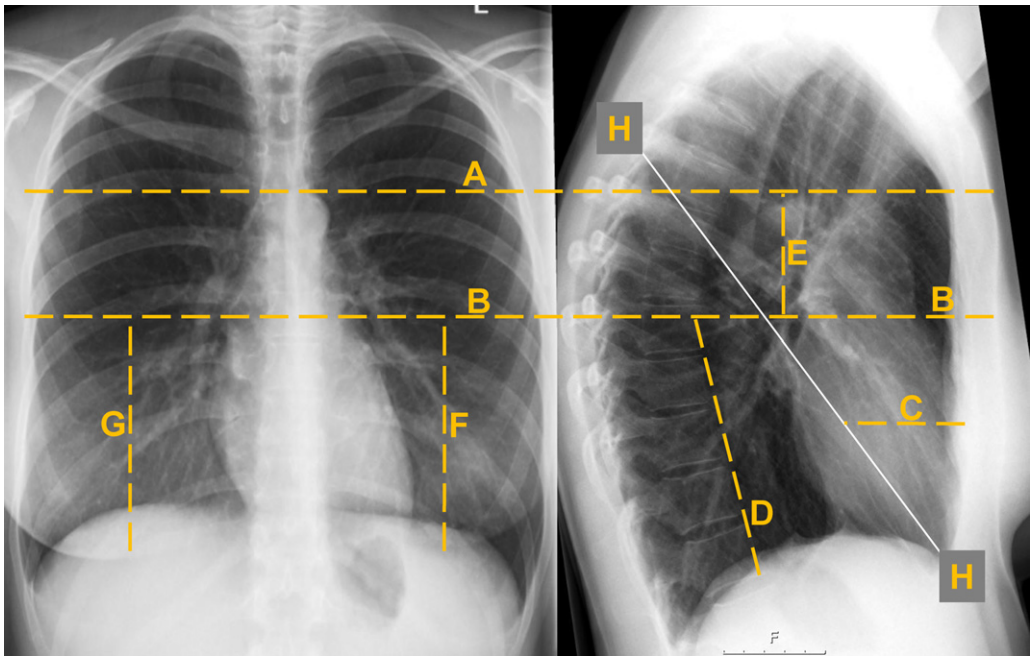

Fig. 1. Modified lung segments. (A) Virtual axial plane through the most cranial point of the aortic arch; (B) virtual axial plane through the cavo-atrial junction; (C) virtual axial plane through the middle of the heart (bisects the heart, cranio-caudal diameter); (D) coronal plane through the ventral spine; (E) coronal plane through the middle of the upper lung (halving the anterior–posterior diameter of the lungs); (F, G) virtual sagittal plane through the middle of the right or left lung (halving the width of each lung). Right lung segments (10) and borders. Upper lobe: 1, apical segment: caudal border = A; 2, posterior segment: cranial border = A, anterior border = E, posterior = H; 3, anterior segment: cranial = A, posterior = E, caudal = B. Middle lobe: 4, lateral segment: posterio-caudal = H, medial = G, cranial = B; 5, medial segment: posterio-caudal = H, lateral = G, cranial = B. Lower lobe: 6, apical segment: anterior = H, caudal = B; 7, medio-basal segment: lateral = F, posterior = D, cranial = B; 8, antero-lateral-basal segment: medial = F, posterior = D, cranial = B; 9, latero-basal segment: anterior = D, medial = F, cranial = B; 10, posterio-basal segment: anterior = D, lateral = F, cranial = B. Left lung segments (8) and borders. Upper lobe: 1,2 apico-posterior segment: the combined segment 1 and 2 of the right lung; 3, anterior segment: cranial border = A, posterior = E, caudal = B; 4, upper lingula segment: cranial = B, caudal = C, posterior = H; 5, lower lingula segment: cranial = C, posterior = H. Lower lobe: 6, apical segment: caudal = B, anterior = H; 7,8 anterio-medial segment: combined segment 7 and 8 of right lung; 9, latero-basal segment: anterior = D, medial = F, cranial = B; 10, posterio-basal segment: anterior = D, lateral = F, cranial = B.

use of low-dose CT is limited when detecting a focal pulmonary abnormality because the observer could miss specific CT features of that lesion that assist in making the correct diagnosis. To test whether the above-mentioned intriguing conclusions from recent simulation studies are relevant to in vivo situations, we made an intra-individual comparison between an low dose CT protocol, at 40 mAs, as suggested by the simulations and with a safety margin of 10 mAs, and an accepted standard-dose CT protocol (150 mAs) to detect and interpret nodular and non-nodular (i.e., ground-glass, interstitial and air-space opacities) focal pulmonary abnormalities in patients referred for chest CT examinations. Recent studies demonstrated the benefit of iterative reconstruction in noise reduction [11,12]. Therefore, iterative reconstruction of a subgroup of these CT-patterns in which the low dose CT with filtered back projection would not detect the pattern was performed in a phantom-study.

2. Materials and methods

Sixty patients (24 men, 36 women, median age 58 years (range 31–82 years), median body weight 75 kg (range 47–119 kg)) were enrolled prospectively in this HIPAA-compliant study between January and April, 2010. The study protocol was approved by the local IRB and written informed consent was obtained. The patients were scheduled for a regular or follow-up CT exam to evaluate pulmonary parenchymal disease: 29 patients for follow-up of lung nodules, 21 patients for pulmonary consolidations of diverse reasons and 10 patients for the assessment of interstitial lung disease.

2.1. Image acquisition

All patients were scanned in the supine position from the lung apex to the base of the chest at withheld full inspiration. No intravenous contrast was administered. Image data were obtained using a dual-energy CT scanner (Somatom Definition Dual Source, Siemens, Erlangen, Germany) with a single-source protocol of 120 kV, pitch 1.2, collimation of 128 mm × 0.6 mm, automated tube current modulation (Care Dose®, Siemens, Erlangen, Germany) and using reference mAs (ref. mAs) to individualize the radiation exposure to patient size. The first scan of 150 mAs was followed by a second low dose scan of 40 mAs. The reconstruction slice thickness was 1 mm, reconstruction interval 0.8 mm, and a 512 × 512 matrix at an edge-enhancing sharp (B46) kernel was applied.

2.2. Lung segment classification

A modified lung-segment classification based on anatomical landmarks [13] (Fig. 1) was used as the basis for image interpretation to facilitate image read out and reduce inter-observer variability.

The lung was divided into two transverse planes: the first at the level of the aortic arch, thus rendering apical and antero-posterior upper lobe segments (modified), and the latter was additionally divided using a coronal plane through half of the upper lobe. The lung below the second transverse plane at the cavo-atrial junction demonstrated all modified lower segments of the lower lobe, which themselves were further divided using a coronal plane along the anterior aspect of the thoracic spine and sagittal plane dissecting the lung equally into postero-basal, antero-basal, latero-basal and

Download English Version:

https://daneshyari.com/en/article/4226030

Download Persian Version:

https://daneshyari.com/article/4226030

Daneshyari.com